EUKARYOTIC CELL, Mar. 2005, p. 516–525 Vol. 4, No. 3
1535-9778/05/$08.00+0 doi:10.1128/EC.4.3.516–525.2005

Cryptic Paraflagellar Rod in Endosymbiont-Containing Kinetoplastid Protozoa

Catarina Gadelha,[1,2]* Bill Wickstead,[1] Wanderley de Souza,[2] Keith Gull,[1] and Narcisa Cunha-e-Silva[2]

Sir William Dunn School of Pathology, University of Oxford, Oxford, United Kingdom,[1] and Instituto de Biofisica Carlos Chagas Filho, Universidade Federal do Rio de Janeiro, Rio de Janeiro, Brazil[2]

Received 8 November 2004/Accepted 24 December 2004

Cilia and flagella are central to many biological processes in a diverse range of organisms. The kinetoplastid protozoa are very appealing models for the study of flagellar function, particularly in the light of the availability of extensive trypanosomatid genome information. In addition to the highly conserved 9 + 2 axoneme, the kinetoplastid flagellum contains a characteristic paraflagellar rod structure (PFR). The PFR is necessary for full motility and provides support for metabolic regulators that may influence flagellar beating. However, there is an intriguing puzzle: one clade of endosymbiont-containing kinetoplastids apparently lack a PFR yet are as motile as species that possess a PFR and are able to attach to the invertebrate host epithelia. We investigated how these organisms are able to locomote despite the apparent lack of PFR. Here we have identified a *PFR1* gene in the endosymbiont-bearing trypanosome *Crithidia deanei*. This gene is expressed in *C. deanei* and is able to partially complement a *pfr1* null mutation in *Leishmania mexicana* cells, demonstrating that the encoded protein is functional. Careful reexamination of *C. deanei* flagellar ultrastructure revealed a greatly reduced PFR missed by many previous analyses. This affirms the PFR as a canonical organelle of kinetoplastids. Moreover, although PFR proteins have been conserved in evolution, primary sequence differences contribute to particular PFR morphotypes characteristic of different kinetoplastid species.

Cilia and flagella are central to many biological processes in a diverse range of organisms. In the order Kinetoplastida—the group of flagellates that include trypanosomatid parasites and bodonids—the flagellum is the classical organelle of motility (42). In parasitic species, the kinetoplastid flagellum has also evolved to be an organelle of attachment to the invertebrate vector, playing a critical role in parasite transmission to the vertebrate host (42). Moreover, recent work shows that the kinetoplastid flagellum is also involved in cell division; positioning of the new flagellum, one of the earliest event in cell duplication, defines the axis of polarity in the dividing cell and the position of the internal organelles (31). Finally, flagellar wave reversal in a Ca^{2+}-dependent manner as an avoidance response has been studied in trypanosomatids (39), suggesting that the flagellum in these species may also be a specialized sensory organelle.

The main component of both cilia and flagella is the axoneme. This microtubule-based organelle was most probably present in the ancestor of all modern eukaryotes and is highly conserved in several deeply diverged lines. In many organisms, the axoneme is augmented by extra-axonemal structures—for example, the fibrous sheath in mammalian spermatozoa and the R-fiber of dinoflagellates. In the Kinetoplastida, a characteristic structure known as the paraflagellar rod (PFR) runs alongside the axoneme to form the flagellum. This PFR is an elegant and stable lattice-like arrangement of protein filaments which is composed of two related major proteins, PFR1 and PFR2 (19), and several minor ones (30, 44).

The PFR appears to be necessary for correct flagellar function in kinetoplastids. In *Trypanosoma brucei*, ablation of PFR2 protein expression by RNA interference disrupts PFR construction and results in cell paralysis (2, 4, 5). Deletion of the *PFR1* and/or *PFR2* genes from *Leishmania mexicana* also prevents the formation of a native PFR structure and produces cells with lower swimming velocities and severe flagellar waveform perturbations (29, 37). Part of these phenotypes may result from the fact that the PFR provides a support for the incorporation of at least two metabolic regulators into the flagellum (34). Interestingly, the electron-dense plaques that form when trypanosomatids attach to invertebrate epithelia contain filaments that appear similar to those of the PFR and appear to originate in the PFR itself (6, 10, 41), leading to the hypothesis that the PFR may be the critical organelle mediating attachment to vector cell surfaces.

However, given these functions, it is intriguing that the possession of the PFR structure does not appear to be universal within kinetoplastids. The members of one particular group of trypanosomatid species (exemplified by *Crithidia deanei*, *C. oncopelti*, *C. desouzai*, *Blastocrithidia culicis*, and *Herpetomonas roitmani*) have been described as lacking a PFR (17). These species also share other ultrastructural features (17), the most obvious of which is possession of an enslaved endosymbiont bacterium (13), most probably the result of a single acquisition in the common ancestor of the above species. Surprisingly, these endosymbiont-harboring species are able to attach to the invertebrate host epithelia (15) and are actively motile (21, 39). The cell movement and the flagellar beating features have

* Corresponding author. Mailing address: Sir William Dunn School of Pathology, University of Oxford, South Parks Road, Oxford OX1 3RE, United Kingdom. Phone: 44 1865 285456. Fax: 44 1865 285691. E-mail: catarina.gadelha@path.ox.ac.uk.

been extensively studied, and they show the same major characteristics as other trypanosomatids (22–24, 39). A detailed description of *C. oncopelti* flagellar beat amplitude and frequency has been compared with that of *C. fasciculata* (which possesses a PFR), and no obvious differences could be seen (3; C. Gadelha and K. Gull, unpublished data).

There is an interesting conundrum here: the kinetoplastid PFR is implicated in both motility and attachment, yet the endosymbiont-bearing trypanosomes are motile and capable of attachment despite the apparent lack of a PFR. Here, we address this dichotomy by asking what has happened to the genes for the major PFR proteins in the endosymbiont-bearing *Crithidia deanei*. We show that this organism possesses a gene encoding PFR1 and that this protein is expressed. Despite some sequence differences, this gene is able to partially rescue a *PFR1* deletion mutation in *Leishmania mexicana*. Furthermore, careful reexamination of the *C. deanei* flagellar ultrastructure revealed a greatly reduced PFR that had been missed by many previous analyses, hence reaffirming the PFR as a canonical organelle of kinetoplastids. Moreover, the data show that small differences in primary sequence between highly conserved PFR proteins may impose many of the differences in morphology characteristic of different kinetoplastid species.

MATERIALS AND METHODS

Cells. Promastigotes of *Leishmania mexicana* wild type (WHO strain MNYC/BZ/62/M379) and *PFR1* deletion mutants (Δ*pfr1*::*NEO* Δ*pfr1*::*HYG*, referred to here simply as Δ*pfr1*) (29) were cultured at 28°C in Medium 199 with Earle's Salts and L-glutamine (Gibco) supplemented with 40 mM HEPES, 5% (vol/vol) fetal bovine serum (Gibco), and 5 μg of hemin per ml. *L. mexicana* complemented cell lines Δ*pfr1*::*NEO* Δ*pfr1*::*HYG* [pNUS-*GFP*cB] (referred to here as Δ*pfr1*[*GFP*]), Δ*pfr1*::*NEO* Δ*pfr1*::*HYG* [pNUS-Lmx*PFR1*cB] (Δ*pfr1*[Lmx]), and Δ*pfr1*::*NEO* Δ*pfr1*::*HYG* [pNUS-Cde*PFR1*cB] (Δ*pfr1*[Cde]) were cultured as above, with the addition of 20 μg of phleomycin (Sigma) per ml. *Crithidia deanei*, *C. oncopelti*, and *C. fasciculata* coanomastigotes and *Herpetomonas megaseliae* promastigotes were grown at 28°C in brain heart infusion medium supplemented with 5% (vol/vol) fetal calf serum. Procyclic *Trypanosoma brucei* 427 cells were cultured at 28°C in SDM 79 medium supplemented with 10% (vol/vol) fetal calf serum.

Gene cloning. We used all publicly available PFR1 and PFR2 sequences to identify conserved regions that could be used to design degenerate oligonucleotides capable of amplifying PFR genes from a wide range of Euglenozoa. Kinetoplastid and euglenoid sequences—namely, sequences from *Crithidia fasciculata* (AY568294 and AY568293), *Leishmania mexicana* (AY198411 and U45884), *Euglena gracilis* (AF044217), *Lepocinclis ovata* (AF296721 and AF263944), *Khawkinea quartana* (AF296722, AF263943, and AF263945), *Gyropaigne lefevrei* (AF263946), *Phacus smulkowskianus* (AF188117 and AF296720), and *Distigma curvatum* (AF188118), and sequence from the genome-sequencing projects for *Leishmania major* (www.sanger.ac.uk/Projects/L_major), *L. infantum* (www.sanger.ac.uk/Projects/L_infantum), *L. braziliensis* (www.sanger.ac.uk), *Trypanosoma brucei* (www.sanger.ac.uk/Projects/T_brucei), *T. congolense* (www.sanger.ac.uk/Projects/T_congolense), *T. vivax* (www.sanger.ac.uk/Projects/T_vivax), *T. b. gambiense* (www.sanger.ac.uk/Projects/T_b_gambiense), and *T. cruzi* (www.tigr.org/tdb/e2k1/tca1)—were aligned. Oligonucleotides 5′-ACGACGCSATCCAGAAGGC and 5′-CTTSGCGTTSGGGTCGAA span a 189-amino-acid (567-bp) fragment (residues 284 to 473 of *T. brucei* PFR1). These were used in PCR with *C. deanei*, *C. oncopelti*, *C. fasciculata*, *H. megaseliae*, or *T. brucei* genomic DNA templates (prepared as described in reference 43). Amplicons from each species were cloned, and several clones were sequenced. *C. fasciculata*, *H. megaseliae*, and *T. brucei* templates generated amplicons encoding fragments of both PFR1 and PFR2 proteins, whereas those from *C. deanei* and *C. oncopelti* gave only PFR1 sequence. For amplification of tandemly repeated *PFR* genes, oligonucleotides 5′-AGCGGCTGGAGGAGAT and 5′-GGTCGCAGTTGTACAC were used. We also used 5′-GTTCCTSGACGTGTG and 5′-CCATGTTGCCGGACTCAAC to specifically amplify *PFR2* sequences. Both of these combinations resulted in *PFR* fragments from *C. fasciculata*, *H. megaseliae*, and *T. brucei* templates but not from *C. deanei* and *C. oncopelti*.

The *C. deanei* central region was used to generate complete *PFR1* mRNA sequence—amplifying from this central region toward both ends by reverse transcription-PCR (RT-PCR). RNA was produced using the High-Pure RNA isolation kit (Roche). First-strand cDNA synthesis used either random hexadeoxynucleotides or oligo$(dT)_{15}$ primers and the Omniscript reverse transcriptase kit (Qiagen). The N terminus was amplified using 5′-AGTTTCTGTACTWTATTG and 5′-GAATTCTAATTGAATATGTGT (crithidial mini-exon sequence), and the C terminus was amplified using 5′-ACGACGCSATCCAGAAGGC and oligo$(dT)_{20}$.

Sequence analysis. Multiple alignments of protein sequences were made using the ClustalW algorithm and manually adjusted as necessary. Phylograms were inferred from these alignments, using both maximum-parsimony (MP) and neighbor-joining (NJ) methods as implemented by the software PAUP*4.0-β10 (Sinauer Associates Inc.). MP trees were built by full heuristic searches with tree-bisection-reconnection (TBR) swapping, and start trees were generated by simple stepwise addition. Gaps were interpreted as missing data. NJ tree inference employed a mean distance measure and an objective of minimum evolution. A total of 100 bootstrap replicates were made for both methods.

Southern blot analysis. DNA transfer to membranes was performed as described elsewhere (43). Fluorescein-labeled probes were generated by random priming (Gene Images kit; Amersham Life Science) from the following unlabeled DNA: Cde*PFR1*, Tbr*PFR1*, Tbr*PFR2*, Lmx*PFR1*, Lmx*PFR2*, Cfa*PFR1*, and Cfa*PFR2*. For cross-species hybridizations, medium-stringency conditions were used: hybridization was performed overnight at 56°C in 0.1% (wt/vol) sodium dodecyl sulfate (SDS), 5% (wt/vol) dextran sulfate–5% (vol/vol) blocking solution (Amersham)–5× SSC (1× SSC is 0.15 M NaCl plus 0.015 M sodium citrate), and blots were washed to a stringency of 0.1% SDS–0.3× SSC at 60°C. Hybridizations with species-specific probes were preformed under high-stringency conditions (hybridized at 60°C overnight as above and then washed to stringency of 0.1% SDS–0.1× SSC at 62°C). Hybridized probe was detected with an anti-fluorescein alkaline phosphatase-conjugated antibody followed by addition of the chemiluminescent substrate CDP-star (Amersham Life Science).

Plasmid construction and transfection of *Leishmania*. The pNUS-GFPcB vector, kindly supplied by E. Tetaud and A. Fairlamb (40), allows the coexpression of an introduced gene (between glutathionylspermidine synthetase 5′ and phosphoglycerate kinase 3′ sequences from *C. fasciculata*) and a phleomycin-resistance marker (*BLE*). pNUS-GFPcB was digested with XhoI, filled in with T4 DNA polymerase, and digested with NdeI to remove the green fluorescent protein fragment. Genomic PCR was used to amplify the Lmx*PFR1* open reading frame (ORF) with 5′-CATATGGATGATGACCCCTGAAGATG and 5′-GATATCAATGCACATACCCTCCAGCT and to amplify the Cde*PFR1* ORF with 5′-CATATGAAAAAGGAAAGAATATGTCT and 5′-GATATCCCTTCATTCTTYTTTCACTT. These amplicons were ligated into the EcoRV site of pBluescriptSK(+), released by NdeI and EcoRV digestion, and ligated into pNUS-GFPcB prepared as described above, yielding plasmids pNUS-LmxPFR1cB and pNUS-CdePFR1cB, respectively. The identity and direction of the introduced fragments was checked by sequencing.

L. mexicana Δ*pfr1* cells were transfected with episomal plasmids by electroporation. Cells were harvested, washed twice in Cytomix (120 mM KCl_2, 0.5 mM $CaCl_2$, 10 mM K_2HPO_4, 10 mM KH_2PO_4, 25 mM HEPES, 2 mM EDTA, 5 mM $MgCl_2$ [pH 7.6]), and resuspended to a final concentration of 5×10^7 cells ml^{-1}. A total of 2.5×10^7 cells were placed in a 4-mm cuvette, and 10 μg of plasmid were added prior to electroporation twice at 1.7 kV with three × 100-μs pulses (Electro Square Porator; BTX). Following transfection, the cells were allowed to recover in normal growth medium for 16 h, after which time transformants were selected with 20 μg of phleomycin per ml. Episome-containing cell lines were maintained as populations in the presence of phleomycin.

Antibodies. Monoclonal antibodies (MAb) used in this study were F4, which recognizes both PFR1 and PFR2 in *Leishmania* spp. (kindly supplied by Diane McMahon-Pratt [26]); L8C4, which recognizes PFR2 in *T. brucei*; and L13D6, which recognizes both PFR1 and PFR2 in *T. brucei* (27) but only PFR1 in *Leishmania* spp. (data not shown).

Immunofluorescence. *L. mexicana* promastigotes were settled onto poly-L-lysine-coated slides and fixed in methanol at −20°C for 10 min. The cells were labeled with L13D6 in phosphate-buffered saline (PBS) (140 mM NaCl, 3 mM KCl, 10 mM sodium phosphate, 2 mM potassium phosphate [pH 7.2]) containing 0.5% (wt/vol) skim milk and visualised with tetramethylrhodamine-5-isothiocyanate (TRITC)-conjugated anti-mouse immunoglobulins (Sigma) in PBS containing 1% (wt/vol) bovine serum albumin. The cells were embedded in Vectashield with DAPI (4′,6-diamidino-2-phenylindole; Vector Laboratories). Cytoskeletons were prepared from live cells settled on slides by extraction with 1% (vol/vol) NP-40 in PEME buffer (100 mM PIPES, 1 mM $MgSO_4$, 0.1 mM EDTA, 2 mM EGTA [pH 6.9]), followed by fixation as above. *C. deanei* cells and cytoskeletons

were prepared as above, with the exception of being fixed in 1% paraformaldehyde in PBS for 5 min.

1D SDS-PAGE and Western blot analysis. For whole-cell protein samples, cells were harvested, washed in PEME buffer with 5 μM E-64d (Sigma), pelleted and immediately resuspended in boiling Laemmli buffer (2% SDS, 10% [vol/vol] glycerol, 400 mM β-mercaptoethanol, 50 mM Tris-HCl [modified pH 7.2]). For detergent fractionation, cells were harvested and washed as above and resuspended in PEME buffer containing 1% (vol/vol) NP-40, 200 μg of DNase I per ml, and protease inhibitors (5 μM E-64d, 10 mM 1,10-phenanthroline, 50 μM leupeptin, 7.5 μM pepstatin A, 500 μM phenylmethylsulfonyl fluoride, 100 μM tosyl-lysyl-chloromethyl ketone [TLCK], 100 μM tolylsulfonyl phenylalanyl chloromethyl ketone [TPCK], 1 mM EDTA [all from Sigma]). The cells were incubated for 5 min on ice and centrifuged at 3,400 × *g* for 15 min at 4°C. Pelleted material was washed once in PEME buffer, and protein in the supernatant was acetone precipitated. Both samples were resuspended in boiling Laemmli buffer and boiled for 5 min. SDS-polyacrylamide gel electrophoresis (PAGE) and immersion transfer to nitrocellulose membrane were performed using standard techniques described elsewhere (36). For immunoblotting, the membranes were blocked with 3% (wt/vol) skim milk in TTBS (20 mM Tris-HCl, 500 mM NaCl, 0.05% Tween 20 [pH 7.5]), labeled with anti-PFR monoclonal antibody with 0.5% skim milk, and developed with horseradish peroxidase-conjugated anti-mouse immunoglobulins (Sigma).

MS. Briefly, SDS-PAGE gels were fixed for 30 min in 10% methanol–5% acetic acid and stained with SYPRO ruby (Sigma). Bands were excised over 280-nm UV light and macerated. Gel fragments were washed in 50% acetonitrile–50 mM ammonium bicarbonate (pH 8.5) solution, dehydrated in 100% acetonitrile, and air dried. Proteins were then digested for 16 h with ~20 μg of trypsin (mass spectrometry [MS] grade; Promega) per ml in 25 mM ammonium bicarbonate at 37°C. Electrospray ionization (ESI)-MS/MS was performed on a Micromass Q-ToF micro instrument (Waters), and masses were analyzed by the MASCOT search engine (Matrix Science).

Electron microscopy. Thin-section transmission electron microscopy (TEM) for *Leishmania* samples was performed by harvesting cells and fixing them in 2.5% glutaraldehyde–2% paraformaldehyde–100 mM sodium phosphate (pH 6.5) for 2 h at 4°C. Samples were postfixed in 1% osmium tetroxide in 100 mM sodium phosphate buffer (pH 6.5) for 1 h at 4°C, washed several times in double-distilled water, en bloc stained with 0.5% aqueous uranyl acetate for 16 h at 4°C, dehydrated through acetone and propylene oxide, and embedded in TAAB 812 embedding resin. *C. deanei* cells were washed in PBS, fixed in 2.5% glutaraldehyde–100 mM sodium phosphate (pH 7.0) for 1 h at room temperature, postfixed in 0.5% osmium tetroxide in 100 mM sodium phosphate buffer (pH 7.0) for 20 min at 4°C, dehydrated through ethanol, and embedded in Spurr (TAAB). Whole-mount cytoskeletons were prepared by settling cells onto carbon-coated, charged Formvar grids, extracting lipids with 1% (vol/vol) NP-40 in PEME buffer, fixing the cells in 2.5% glutaraldehyde in PEME buffer, and negatively staining them with 0.7% gold-thioglucose in water.

Motility analysis. *L. mexicana* cell lines were grown to a density of 5×10^6 cells ml^{-1} and equilibrated to 22°C for 1 h. These cells (in medium) were placed onto slides and covered with a glass coverslip raised above the slide surface with 50-μm-thick tape (ca. two cell lengths). To prevent cell adherence, both slide and coverslip were precoated with poly-L-glutamate. The edges of the coverslip were then sealed to avoid capillary flow of liquid. Time-lapse sequences of images captured every 1 s for 1 min were made at 22°C and low magnification (10×) using phase-contrast illumination. For each cell line, velocity measurements (assuming movement along the *z*-axis to be negligible) were made by tracking ~100 cells over all 60 frames.

Nucleotide sequence accession numbers. Sequence data reported here are available from GenBank under accession numbers AY785777, AY785778, AY785779, and AY785780.

RESULTS

***C. deanei* possesses a gene encoding PFR1.** To determine whether an endosymbiont-containing organism (apparently not possessing a PFR) possesses any putative *PFR* genes, we designed degenerate oligonucleotides which were able to amplify both *PFR1* and *PFR2* genes from any trypanosomatid species. PCR from genomic DNA of *C. deanei* amplified a *PFR* gene fragment. To complete the sequence of this gene fragment and to test for transcription, we performed RT-PCR on *C. deanei* RNA, using either crithidial mini-exon or poly(T) primers along with *PFR*-specific primers. This revealed a full-length, fully processed mRNA that clearly encoded a homologue of a major PFR protein (Fig. 1A). We used the same strategy to isolate a *PFR* gene from the endosymbiont-bearing species *C. oncopelti* and genes from the nonendosymbiont-bearing trypanosomes *C. fasciculata* and *H. megaseliae* and, as a control, the previously described genes of *T. brucei*.

Figure 1A shows an alignment of the putative PFR protein from *C. deanei* with PFR1 and PFR2 from *T. brucei* and *L. major*. The encoded protein is 591 amino acids in length and has a predicted pI of 5.28—consistent with other known major PFR proteins. Phylogenetic analyses showed unambiguously that the proteins encoded by the endosymbiont-bearing species (*C. deanei* and *C. oncopelti*) are PFR1 orthologues (Fig. 1B). In contrast, both PFR1 and PFR2 sequences were isolated from *C. fasciculata*, *H. megaseliae*, and *T. brucei*.

***C. deanei PFR1* is a single copy gene.** To date, the major PFR protein genes have been found to be present as tandemly duplicated arrays in all the kinetoplastids for which information is available (Table 1). This is thought to be a consequence of a need for high levels of mRNA from these genes. The newly identified *C. deanei* PFR gene (Cde*PFR1*) was used as a probe in Southern hybridization to restriction endonuclease-digested *C. deanei* genomic DNA in an assay of gene copy number. This showed that *C. deanei PFR1* is a single-copy gene (data not shown), in comparison to the multiple copies present in endosymbiont-lacking species. This conclusion was reinforced by the results of a strategy to amplify tandemly repeated *PFR* genes, which produced amplicons from the species with multiple copies of *PFR1*, but not from *C. deanei* or *C. oncopelti* (data not shown).

Complementation experiments. Phylogenetic inference using a maximum-parsimony method indicates that CdePFR1 protein has accumulated a greater number of changes since the last common ancestor than have PFR1 proteins from endosymbiont-lacking species (as shown by the branch lengths in Fig. 1B). We addressed whether CdePFR1 is a functional PFR protein (in spite of sequence divergence) by using a complementation approach. Maga et al. (29) have previously described the *L. mexicana* double-gene-knockout line Δ*pfr1*::NEO Δ*pfr1*::HYG—referred to here simply as Δ*pfr1*— which does not assemble a native PFR structure and shows severely reduced swimming motility. We complemented this cell line with an episomal copy of either *C. deanei* or *L. mexicana PFR1*, to produce cell lines Δ*pfr1*[Cde] and Δ*pfr1*[Lmx], respectively.

We used the MAb L13D6 (which recognizes both PFR1 and PFR2 in *T. brucei* but only PFR1 in *Leishmania* spp.) to check for PFR1 expression and correct localization in complemented cell lines. In these immunofluorescence experiments, a bright signal was observed along the entire flagellum of wild-type and both complemented cell lines, Δ*pfr1*[Cde] and Δ*pfr1*[Lmx] (Fig. 2A). This signal was also seen in cells that had been detergent extracted to produce cytoskeletons, demonstrating a tight association with the axoneme (data not shown). These results show the correct targeting and incorporation of CdePFR1 into the flagellar cytoskeleton of *L. mexicana*.

Given that CdePFR1 protein assembles into the *Leishmania* PFR structure in complemented cells and remains associated on detergent extraction, we then asked if it was able to recruit

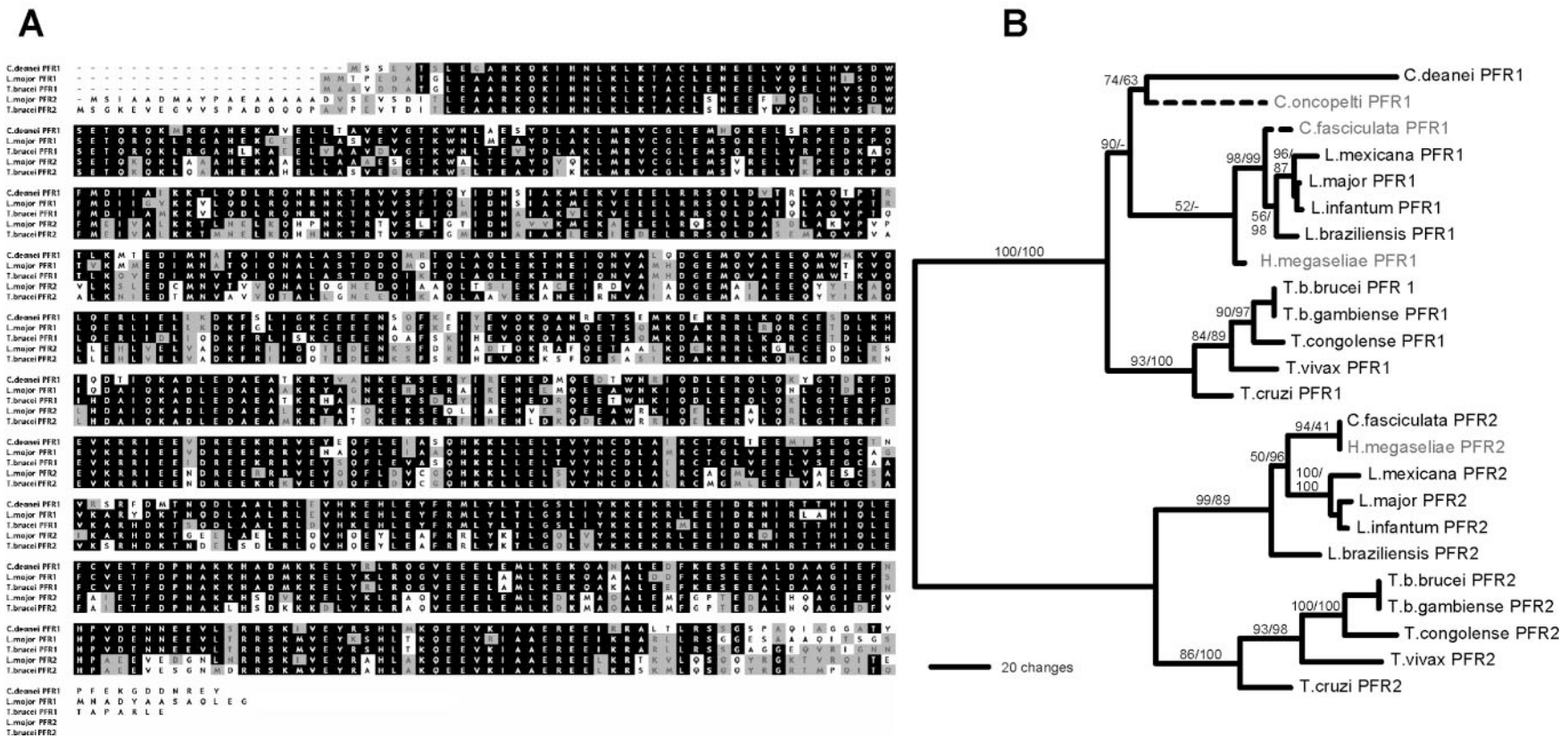

FIG. 1. *C. deanei* possesses a gene encoding PFR1. (A) Alignment of the major PFR proteins from *C. deanei*, *L. major*, and *T. brucei.* Black shading indicates identical residues, and grey shading indicates similar residues. (B) Phylogenetic analysis of PFR sequences of Kinetoplastida. The MP unrooted phylogram shown was inferred from protein alignments. Topology support from 100 bootstrap replicates using either MP or NJ methods are shown next to nodes (MP/NJ). Partial sequences are shown in grey.

TABLE 1. Distribution of *PFR1* copy number across the Kinetoplastida

Species (strain)	*PFR1* copy no.[a]	Reference
T. brucei (927)	5	www.sanger.ac.uk/Projects/T_brucei
T. brucei (427)	4	11
L. major	3	www.sanger.ac.uk/Projects/L_major
L. mexicana	4	29
H. megaseliae	≥2	This study
C. fasciculata	≥2	This study
C. oncopelti	1	This study
C. deanei	1	This study

[a] Copy number per haploid genome.

other PFR proteins to the structure. SDS-PAGE and Western blot analysis using MAb F4 (which recognizes both PFR1 and PFR2 in *Leishmania* spp.) were performed on whole-cell lysates and detergent-soluble and -insoluble fractions from *L. mexicana* cells lines. In the absence of PFR1 in the deletion mutant Δ*pfr1*, PFR2 accumulates mostly in the detergent-soluble fraction (Fig. 2B). However, when PFR1 is expressed in the complemented strains, PFR2 is recruited to the cytoskeleton fractions, although some remains detergent soluble. This is true of both Δ*pfr1*[Lmx] and Δ*pfr1*[Cde] complemented lines (Fig. 2B). Therefore, not only is CdePFR1 incorporated into the leishmanial Δ*pfr1* cytoskeleton but also it enables the re-

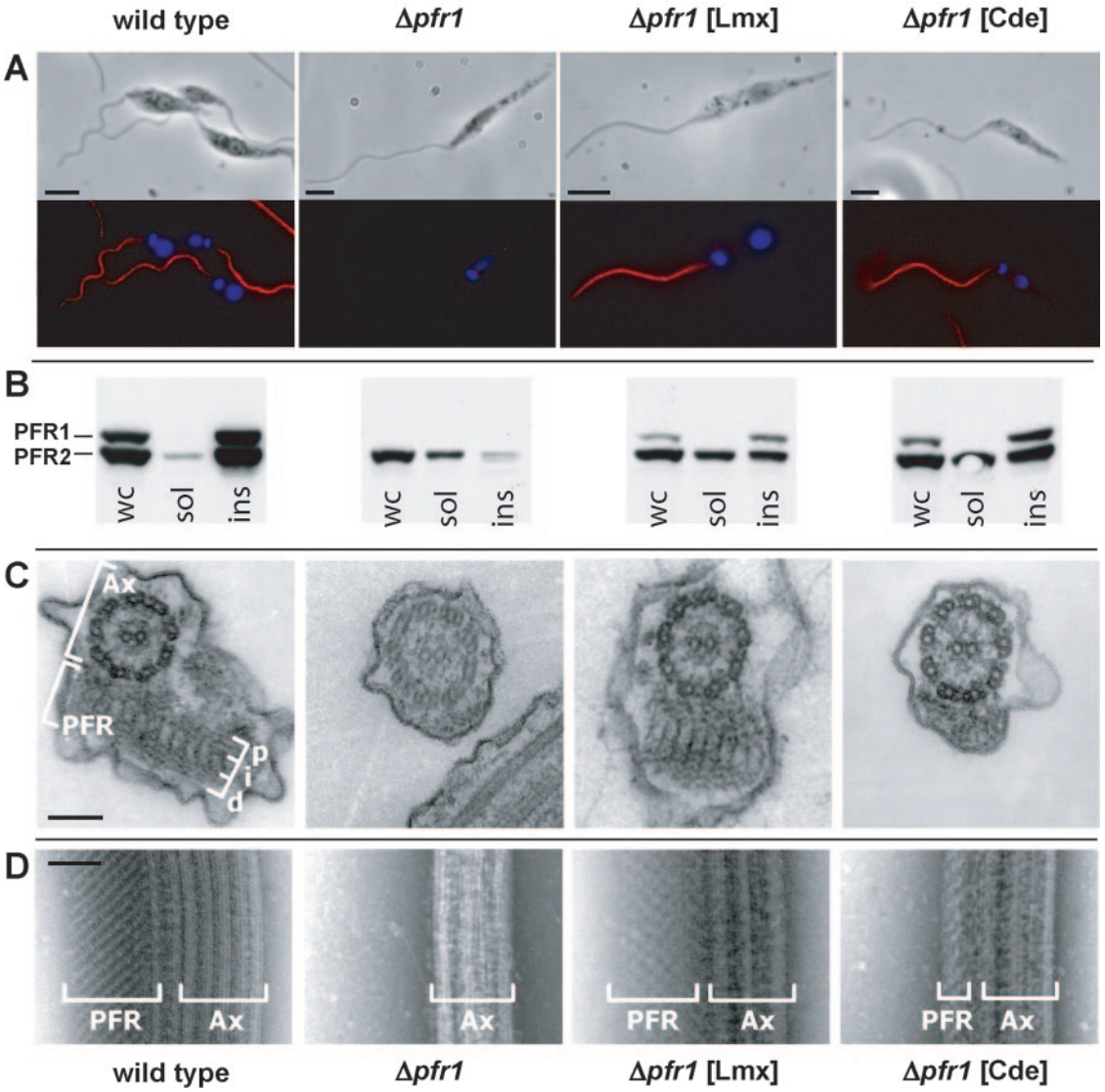

FIG. 2. Cells complemented with *C. deanei* PFR1 build a PFR structure of reduced thickness that incorporates endogenous PFR2. Wild-type *L. mexicana* samples are shown alongside *PFR1* deletion mutants (Δ*pfr1*) and mutants complemented with *L. mexicana PFR1* (Δ*pfr1*[Lmx]) and *C. deanei PFR1* (Δ*pfr1*[Cde]). (A) Phase-contrast microscopy and corresponding immunofluorescence images. DNA is labeled with DAP1 (blue), and the PFR is identified by the L13D6, anti-PFR1 MAb (red). Scale bars, 5 μm. (B) Western blot analysis of cell lines. Protein samples from 2×10^7 cells were separated by SDS-PAGE and analyzed with MAb F-4, which recognizes both-PFR1 and PFR2 in *Leishmania* spp. Whole-cell protein (wc) was separated alongside cell equivalents of detergent-soluble (sol) and insoluble (ins) fractions. (C) Thin-section TEM of flagella from the cell lines. The positions of the axoneme (Ax) and three domains of the PFR—proximal (p), intermediate (i), and distal (d)—are indicated on the wild-type. Scale bar, 200 nm. (D) Negatively stained whole-mount cytoskeletons of complemented cell lines. Axoneme (Ax) and PFR structures are indicated. Scale bar, 200 nm.

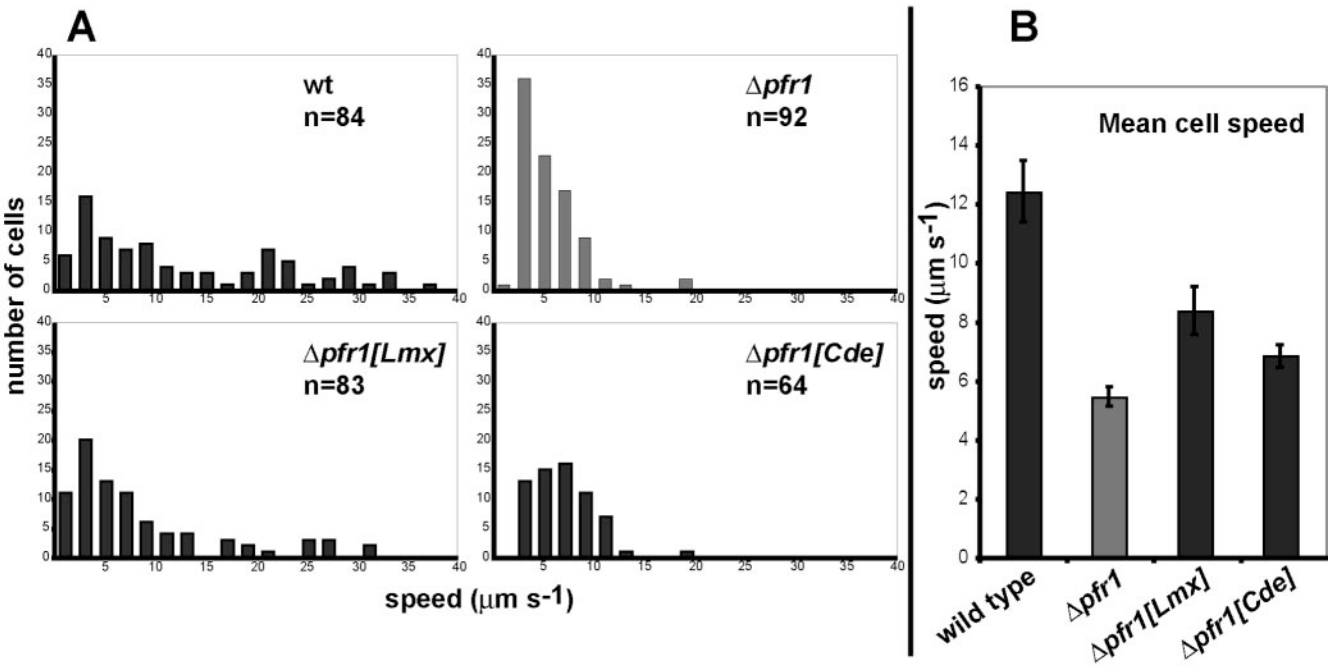

FIG. 3. *C. deanei PFR1* partially rescues the *L. mexicana* Δ*pfr1* motility defect. (A). Distribution of cell speeds for wild-type (wt), Δ*pfr1*, Δ*pfr1*[Lmx], and Δ*pfr1*[Cde] cell lines. Speeds shown are mean for each cell (of *n* total) over a 60-s period. (B) Mean speeds of cell lines. Standard errors are represented by bars.

cruitment of endogenous LmxPFR2 to the flagellum. These results are consistent with the model of PFR organization (29), in which PFR1 and PFR2 are present throughout the structure although only PFR1 is involved in attachment to the axoneme.

TEM of thin sections and whole-mount cytoskeletons was used to identify the level of structural organization of the assembled PFR within the flagellum of complemented cell lines. Seen in cross-section, the PFR of wild-type cells consists of three ultrastructural domains, named the proximal, intermediate, and distal domains in order of increasing distance from the central axis of the axoneme (Fig. 2C). The proximal domain is connected via bridges to axonemal doublets 4 to 7, maintaining the tight association of axoneme and PFR. In the deletion mutant Δ*pfr1*, the main PFR structure was absent and only the connecting bridges to the axoneme were seen (Fig. 2C and D). This phenotype is rescued in the Δ*pfr1*[Lmx] strain, where a wild-type PFR was observed in the flagellum. In Δ*pfr1*[Lmx] cells, all three domains of the PFR were restored. Interestingly, although the deletion mutant complemented with the *C. deanei* PFR1, Δ*pfr1*[Cde], constructed a major portion of the PFR, the structure lacked much of the detailed intermediate and distal organisation seen in wild-type *Leishmania* and Δ*pfr1*[Lmx] cells ($n > 100$; Fig. 2C and D).

Wild-type *L. mexicana* swims actively in culture. On the other hand, *L. mexicana PFR* null mutants—Δ*pfr1* and Δ*pfr2*—display severe reduction in flagellar and cellular motility (28). Having seen that the *C. deanei* PFR1 could enable the elaboration of a substantial PFR in the *Leishmania* null mutant, Δ*pfr1*, we next asked if this endowed the cells with increased mobility. We used time-lapse microscopy to monitor the cellular motility of the *L. mexicana* cell lines produced here. Figure 3 shows the distribution of individual cell speeds and also the mean speeds for each cell line. These data show that expression of episomally encoded LmxPFR1 in Δ*pfr1*[Lmx] essentially rescues the defective motility phenotype (two-sample unpaired *t* test; Δ*pfr1*[Lmx] versus Δ*pfr1* mean speed; $P = 0.002$), although the full wild-type mean speed could not be reached (Δ*pfr1*[Lmx] versus wild type; $P = 0.003$). Expression of CdePFR1 also significantly increased cellular motility (Δ*pfr1*[Cde] versus Δ*pfr1*; $P = 0.006$). Interestingly, the mean cell speeds of Δ*pfr1*[Lmx] and Δ*pfr1*[Cde] were not significantly different ($P = 0.11$), despite Δ*pfr1*[Cde] cells clearly not being able to reach the same maximal speeds as Δ*pfr1*[Lmx] cells (as shown by the distribution in Fig. 3A).

The results shown here indicate that the endosymbiont-bearing kinetoplastid *C. deanei*—previously described as lacking a PFR—encodes a functional, expressed PFR1 protein that possesses all necessary information to be transported and incorporated into the flagellar cytoskeleton of the PFR-containing species *L. mexicana*. CdePFR1 interacts with the axoneme-connecting bridges and recruits endogenous LmxPFR2 to assemble a PFR structure, albeit reduced in thickness and intermediate and distal organization compared to that of *Leishmania* itself. In addition, this structure is able to partially rescue the motility defect of *L. mexicana PFR1* deletion mutants.

The crithidial PFR. The functional expression of CdePFR1 in an exogenous system and the knowledge that its RNA was present in *C. deanei* cells clearly raised the issue of whether the CdePFR1 protein was actually expressed in *C. deanei*. A single band of CdePFR1 was detected by Western blot analysis using the MAb L13D6 against whole-cell and detergent-insoluble protein preparations (Fig. 4A). To exclude the possibility of cross-reactivity with an epitope-containing unrelated protein,

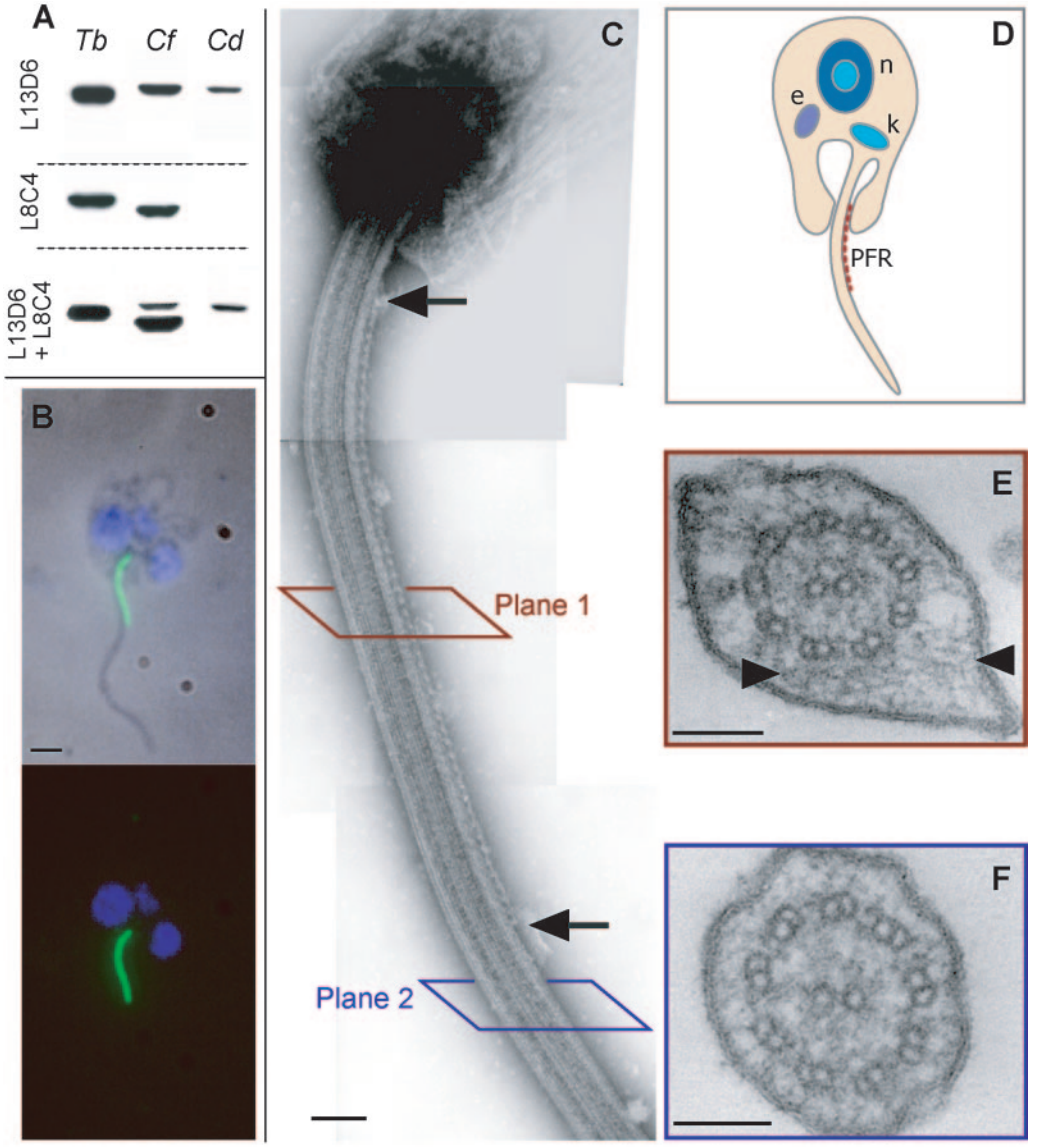

FIG. 4. The PFR of *C. deanei.* (A) Western blot analysis of major PFR proteins. Protein samples from 0.5×10^7, 1×10^7, and 2×10^7 cytoskeletons of *T. brucei*, *C. fasciculata*, and *C. deanei*, respectively, were separated by SDS-PAGE and analysed with MAb L13D6 (reacts with PFR1 in *Crithidia* spp. and with PFR1 and PFR2 in *T. brucei*) or MAb L8C4 (reacts with PFR2 only). A Western blot using both MAbs together is also shown. Note that PFR1 and PFR2 of *T. brucei* are not resolved on these blots. (B) Phase-contrast microscopy and corresponding immunofluorescence image for a *C. deanei* coanomastigote. DNA is labeled with DAPI (blue), and the PFR is identified by MAb L13D6 (green). Scale bars, 1 μm. (C) Ultrastructure of *C. deanei* PFR visualized by TEM of negatively stained whole-mount cytoskeletons. Arrows show the limits of the PFR structure along the flagellum. Scale bar, 200 nm. (D) Schematic representation of *C. deanei* showing the position of the PFR (also the kinetoplast [k], nucleus [n] and endosymbiont [e]). (E and F) TEM on thin sections reveal a putative PFR structure (arrowheads) in some sections (E), but much of the flagellum is free of PFR (F). Scale bars, 100 nm.

the 75-kDa band detected in *C. deanei* cytoskeletons was sequenced by ESI-MS/MS. The peptide sequences obtained were all consistent with the predicted protein of the Cde*PFR1* ORF (Fig. 1A).

The same L13D6 antibody was used in immunofluorescence analysis to label *C. deanei*. A strong signal was detected from inside the flagellar pocket up to the first third of the flagellar length in all cells observed (Fig. 4B). Notably, this flagellar signal was sensitive to the long fixation times (>5 min) and higher concentrations of cross-linking fixatives (>2% paraformaldehyde) that are often used for immunofluorescence. For that reason, we used fixation conditions that did not preserve cell morphology as well as other methods (see Materials and Methods) but allowed the detection of a PFR signal in *C. deanei*.

We then carefully reexamined the ultrastructure of the flagellum in *C. deanei*. Analysis of negatively-stained whole-mount cytoskeletons was most informative (Fig. 4C). These images revealed that this species does indeed posses a PFR. It is, however, much reduced in width and length compared to that of endosymbiont-lacking kinetoplastids and can be visualised in these negatively stained preparations extending along

one side of the flagellum as a thin punctuate line. Importantly, the length and position of the *C. deanei* PFR are consistent with the length of the paraflagellar signal seen by immunofluorescence (Fig. 4B). This much reduced form explains why many previous thin-section studies concluded that the PFR was absent. Thin cross sections of the flagellum along most of its length (e.g., plane 2 in Fig. 4C) should produce images of flagella lacking PFR, as in Fig. 4F (representative of 33 of 41 cross sections). Only when we searched more thoroughly did we obtain flagellar cross sections that exhibited a small extra-axonemal structure that we interpret as being the reduced crithidial PFR (8 of 41 cross sections). This structure is much less obvious than the unambiguous structure seen by negative staining but is always between microtubule doublets 4 and 7 and is attached to the axoneme by putative connecting bridges (Fig. 4E).

PFR2 appears to be absent from endosymbiont-bearing species. Alongside our identification of *PFR1* sequences from *C. deanei* and *C. oncopelti*, we also undertook an extensive search for *PFR2* in these organisms. A large number of techniques were employed (a more detailed account of each can be found in the relevant section of Materials and Methods). PCR from genomic DNA, using degenerate PFR primers, resulted in amplicons of both *PFR1* and *PFR2* fragments from *C. fasciculata*, *H. megaseliae*, and *T. brucei* templates (number of independent clones *PFR1:PFR2-Cf* 4:3, *Hm* 7:5, *Tb* 3:3), but produced only *PFR1* fragments from *C. deanei* and *C. oncopelti* (*Cd* 11:0, *Co* 6:0). Similar results were achieved in RT-PCR experiments using different primer sets (*Cf* 0:14, *Tb* 4:2, *Cd* 24:0, *Co* 5:0). Moreover, two sets of *PFR2*-specific primers produced amplicons when used with *C. fasciculata*, *H. megaseliae*, and *T. brucei* gDNA templates, but not with *C. deanei* or *C. oncopelti*. Southern blot analyses using *T. brucei*, *L. mexicana*, and *C. fasciculata PFR2* coding regions as probes could easily identify *PFR2* sequences in gDNA from each of *C. fasciculata*, *H. megaseliae*, and *T. brucei* (i.e., even when Lmx*PFR2* was used to probe for Tbr*PFR2*) but did not unambiguously identify a sequence in *C. deanei* or *C. oncopelti* gDNA (data not shown).

Searches for PFR2 protein showed similar results to those for the *PFR2* gene. A MAb specific for PFR2 protein (L8C4; Fig. 4A) produced no strong reaction to protein samples from *C. deanei* and *C. oncopelti* separated by SDS-PAGE. An antibody reacting with both PFR1 and PFR2 proteins in most species (MAb F4 [26]), produced a strong reaction to only one band in one-dimensional SDS-PAGE with protein samples from *C. deanei* and *C. oncopelti*. Furthermore, protein sequencing from one-dimensional SDS-PAGE and also two-dimensional electrophoresis demonstrated that both major PFR proteins could be found in *C. fasciculata* and *T. brucei* protein preparations. In *C. deanei* protein samples, the strongly reacting band contained PFR1 protein, as expected, whereas taking weakly reacting bands revealed only abundant, unrelated proteins (Hsp70 and Hsp80). Each of the above techniques has limitations. However, taken together, it is very striking that we have found no evidence for the presence of PFR2 protein nor encoding DNA or RNA in kinetoplastid species that harbor the endosymbiont.

DISCUSSION

Evolutionary distribution of the PFR. The PFR is an extra-axonemal structure that appears to be restricted to the sister orders Kinetoplastida and Euglenida. Dinoflagellates were once included in the PFR-containing group because of the presence of an extra-axonemal structure within the flagellum. However, these structures do not resemble the paracrystalline PFR of kinetoplastids and euglenoids. In addition, these two groups of excavate protozoa are phylogenetically distinct from the dinoflagellates (phylum Alveolata), from which they diverged very early in eukaryote evolution (8). At present, no sequence is available for proteins of the dinoflagellate paraaxial structure; however, it is most probable that this structure and the PFR are examples of convergent, rather than divergent, evolution, since it is known that extra-axonemal structures have evolved independently several times across eukaryotes.

Previous structural studies have reported a lack of PFR in kinetoplastids possessing an endosymbiotic bacterium (12, 17). During the early phases of the identification of PFR1 and PFR2 in *T. brucei*, one antibody used gave a weak Western blot signal to proteins of *C. deanei* but not *C. oncopelti* (38). The suggestion was made, therefore, that if this signal was from a bona fide PFR protein, it was not incorporated into a structural entity (38). There are, of course, many explanations for such discrepant observations. Here, we have resolved this issue by demonstrating that the endosymbiont-bearing *C. deanei* does indeed possess a gene encoding a major PFR protein (PFR1) and that this protein is recognized by antibodies raised to PFR proteins from other species. Moreover, this protein forms part of a flagellar structure in *C. deanei* that, although reduced, is undoubtedly recognizable as a PFR.

It is worth noting that the PFR1 phylogeny shown here agrees with those inferred from other molecular data (14, 20) in supporting the monophyly of the endosymbiont-bearing species (as would be expected for a rare event such as enslavement). Our phylogeny, in common with the rRNA data (20), also suggests that non-endosymbiont-bearing *Crithidia* species diverged from those possessing an endosymbiont soon after the divergence of the leishmanial and trypanosomal lines and that the nomenclature of the kinetoplastids often does not reflect evolutionary relatedness (for example, the genera *Crithidia* and *Herpetomonas* encompass both endosymbiont-bearing and endosymbiont-lacking species and are not monophyletic taxa).

PFR structural organization. Visualized by thin-section TEM, the PFR consists of three morphologically distinct regions. These are named the proximal, intermediate, and distal domains, according to their position relative to the axoneme in cross section (Fig. 2C). There are some variations in form, size, and arrangement, but overall the PFRs of all kinetoplastids exhibit a very similar tripartite pattern of construction (1, 16, 18). The PFR has a permanent position relative to the flagellum axoneme, with the proximal region linked to axonemal doublets 4 through 7. Genetic ablation of the major PFR proteins of the *L. mexicana* flagellum has yielded a set of structural assembly rules (29). (i) The connecting bridges that link the PFR to the axoneme do not contain either PFR1 or PFR2, and they assemble in the absence of a native PFR

structure. A possible component of these bridges in *T. brucei* is the protein I_{17}, which has been detected between the PFR and the axoneme (25). (ii) PFR1 is expressed and targeted to the flagellum in the absence of PFR2, where it forms stable associations with axoneme-connecting bridges. (iii) PFR2 is targeted to the flagellum but cannot be assembled into the PFR in the absence of PFR1. (iv) PFR2 incorporation is required for the subsequent assembly of the intermediate and distal domains. (v) PFR1 and PFR2 are present in each of the three domains of the PFR.

Episomal complementation of *L. mexicana PFR1* deletion mutants with *C. deanei PFR1* allowed the localization of CdePFR1 along the length of the flagellum in a manner similar to that of LmxPFR1. In these cells, CdePFR1 was stably bound to the axoneme and was able to stably recruit endogenous LmxPFR2. However, *L. mexicana* Δ*pfr1*[CdePFR1] cells were not able to build full PFR structures; they lacked the intermediate and distal domains. This indicates that, in *Leishmania*, PFR1 not only binds to the axonemal bridges as described above but also is necessary for the construction of the PFR intermediate domain. This second function is evidently not merely a product of PFR binding, because CdePFR1 retains this function. Moreover, the processes of binding to axonemal bridges and seeding (in the presence of PFR2) the construction of the intermediate domain are at least partially independent, since the CdePFR1 protein is able to substitute in the former, but not in the latter.

Wild-type *C. deanei* cells build a reduced PFR that lacks intermediate and distal domains. In these cells, the proximal domain is also much smaller than those of *Leishmania* or *Trypanosoma* species. Interestingly, although we could readily identify a homologue of PFR1 in *C. deanei*, we found no evidence of PFR2 when using a wide variety of techniques. Moreover, in terms of ultrastructure, the PFR of *C. deanei* is not like that formed in *L. mexicana* Δ*pfr1*[CdePFR1] but is reminiscent of the residual structure formed in *L. mexicana PFR2* deletion mutants. Hence, the cryptic nature of the PFR of endosymbiont-bearing kinetoplastids appears to be linked to the selective loss of *PFR2* (but retention of *PFR1*).

The major proteins of the PFR are highly conserved within the kinetoplastids. Despite this, the exact ultrastructure of the PFRs varies from species to species. Our data demonstrate that (in addition to likely major gene losses such as in the endosymbiont-containing kinetoplastids) small variations in the PFR primary sequence can result in significant changes in the overall PFR structure.

PFR function. From the data presented here, we propose that the cryptic PFR built by *C. deanei* is sufficient to perform the functions common to all kinetoplastids, namely, motility and attachment to the invertebrate host epithelium. Expression of *C. deanei* PFR1 in *L. mexicana* Δ*pfr1* cells was able to rescue the motility defect of the null cells. However, this rescue was only partial: complemented cells moved faster than did Δ*pfr1* cells but did not achieve the rates of movement seen in the fastest wild-type cells. This may simply be the result of expressing a nonoptimal version of PFR1, but it is tempting to speculate that it could be linked to the lack of intermediate and distal PFR domains.

It has been shown recently that the PFR is not simply an architectural attribute but, rather, acts as a matrix into which enzymes such as adenylate kinases (34) and calmodulin (35) can be built. These proteins, and possibly many others, are thought to regulate the metabolic environment of the flagellum. Given the small diameter and reduced structural complexity of the *C. deanei* PFR, one may ask whether the PFR in species with an endosymbiont can provide an adequate platform for such regulatory enzymes. If this is the case, how can the crithidial flagellum perform the same functions as in any other kinetoplastid?

One obvious candidate to consider when looking for metabolic alterations is the endosymbiont. This organelle carries sufficient information to code for a complex set of proteins, and it is capable of independent protein synthesis (33). Moreover, it relieves the host cell from dependence on exogenous heme (9), ornithine metabolism enzymes (7), purines, and various amino acids (32). Therefore, it seems plausible that the endosymbiont could compensate the host with some enzymatic functions that would allow the loss of all but a rudimentary PFR. However, when making such suggestions, it must be remembered that both possession of the endosymbiont and lack of a full PFR are traits in the kinetoplastids restricted to a single clade. Since both are monophyletic, the two may result from entirely independent events.

Novel PFR components. Until recently, little progress has been made in the molecular identification of minor PFR components. In this regard, comparative proteomic approaches hold much promise—a comparison of *T. brucei* cells with and without ablation of PFR2 by RNA interference has recently been employed to identify four novel PFR components including the adenylate kinases previously mentioned (34). The creation in this study of a complemented cell line (Δ*pfr1*[Cde]) that builds a proximal domain but no intermediate or distal domains may be a valuable tool in a more detailed description of PFR composition.

Whilst demonstrating that the extra-axonemal PFR is not absent in endosymbiont-bearing kinetoplastids (as previously reported [12, 17]) and that this organelle is therefore most probably universal in the kinetoplastids and euglenoids, we have been able to provide further insights into the relationship of molecular diversity and PFR morphotypes in these fascinating protists.

ACKNOWLEDGMENTS

We thank Diane McMahon-Pratt for the MAb F4, Emmanuel Tetaud and Alan H. Fairlamb for pNUS-GFPcB, David Woolley and Paulo Marcio de Faria e Silva for valuable discussion, Sue Vaughan for help with TEM micrographs, and Ben Thomas for ESI-MS/MS analyses.

This work is supported by grants from the Wellcome Trust, CNPq, and PRONEX-MCT, Brasil. K.G. is a Wellcome Trust Principal Research Fellow. C.G. is supported by CAPES, Brasil.

REFERENCES

1. **Al-Shammary, R. J., N. M. Shoukrey, S. E. Al-Shewemi, E. A. Ibrahim, M. A. Al-Zahrani, and A. S. Al-Tuwaijri.** 1995. *Leishmania major: in vitro* ultrastructural study of the paraxial rod of promastigotes. Int. J. Parasitol. **25:** 443–452.
2. **Bastin, P., T. Sherwin, and K. Gull.** 1998. Paraflagellar rod is vital for trypanosome motility. Nature **391:**548–548.
3. **Bastin, P., A. Bagherzadeh, K. R. Matthews, and K. Gull.** 1996. A novel epitope tag system to study protein targeting and organelle biogenesis in *Trypanosoma brucei*. Mol. Biochem. Parasitol. **77:**235–239.
4. **Bastin, P., T. J. Pullen, T. Sherwin, and K. Gull.** 1999. Protein transport and flagellum assembly dynamics revealed by analysis of the paralysed trypanosome mutant snl-1. J. Cell Sci. **112:**3769–3777.

5. **Bastin, P., T. J. Pullen, F. F. Moreira-Leite, and K. Gull.** 2000. Inside and outside of the trypanosome flagellum: a multifunctional organelle. Microbes Infect. **2:**1865–1874.
6. **Brooker, B. E.** 1971. Flagellar attachment and detachment of *Crithidia fasciculata* to the gut wall of *Anopheles gambiae*. Protoplasma **73:**191–202.
7. **Camargo, E. P., and E. Freymuller.** 1977. Endosymbiont as supplier of ornithine carbamoyl transferase in a trypanosomatid. Nature **270:**52–53.
8. **Cavalier-Smith, T., and E. E.-Y. Chao.** 2003. Phylogeny of Choanozoa, Apusozoa, and other Protozoa and early eukaryote megaevolution. J. Mol. Evol. **56:**540–563.
9. **Chang, K.-P., and W. Trager.** 1974. Nutritional significance of symbiotic bacteria in two species of the hemoflagellates. Science **183:**531–532.
10. **Current, W. L.** 1980. *Cryptobia* sp. in the snail *Triadopsis multilineata* (Say): fine structure of attached flagellates and their mode of attachment to the spermatheca. J. Protozool. **27:**278–287.
11. **Deflorin, J., M. Rudolf, and T. Seebeck.** 1994. The major components of the paraflagellar rod of *Trypanosoma brucei* are two similar, but distinct proteins which are encoded by two different gene loci. J. Biol. Chem. **269:**28745–28751.
12. **de Souza, W., and M. C. M. Motta.** 1999. Endosymbiosis in protozoa of the Trypanosomatidae family. FEMS Microbiol. Lett. **173:**1–8.
13. **Du, Y., G. McLaughlin, and K.-P. Chang.** 1994. 16S ribosomal DNA sequence identities of β-proteobacterial endosymbiont in three *Crithidia* species. J. Bacteriol. **176:**3081–3084.
14. **Du, Y., D. A. Maslov, and K.-P. Chang.** 1994. Monophyletic origin of β-division proteobacterial endosymbionts and their coevolution with insect trypanosomatid protozoa *Blastocrithidia culicis* and *Crithidia* spp. Proc. Natl. Acad. Sci. USA **91:**8437–8441.
15. **Fampa, P., M. S. Correa-da-Silva, D. C. Lima, S. M. P. Oliveira, M. C. M. Motta, and E. M. B. Saraiva.** 2003. Interaction of insect trypanosomatids with mosquitoes, sand fly and the respective insect cell lines. Int. J. Parasitol. **33:**1019–1026.
16. **Farina, M., M. Attias, T. Souto-Padron, and W. de Souza.** 1986. Further studies on the organization of the paraxial rod of trypanosomatids. J. Protozool. **33:**552–557.
17. **Freymuller, E., and E. P. Camargo.** 1981. Ultrastructural differences between species of trypanosomatids with and without endosymbiont. J. Protozool. **28:**175–182.
18. **Fuge, H.** 1969. Electron microscopic studies of the intraflagellar structures of trypanosomes. J. Protozool. **16:**160–166.
19. **Gadelha, C., J. H. LeBowitz, J. Manning, T. Seebeck, and K. Gull.** 2004. Relationships between the major kinetoplastid paraflagellar rod proteins: a consolidating nomenclature. Mol. Biochem. Parasitol. **136:**113–115.
20. **Hollar, L., J. Lukes, and D. A. Maslov.** 1998. Monophyly of endosymbiont containing trypanosomatids: phylogeny versus taxonomy. J. Eukaryot. Microbiol. **45:**293–297.
21. **Holwill, M. E.** 1965. The motion of *Strigomonas oncopelti*. J. Exp. Biol. **42:**125–137.
22. **Holwill, M. E., and J. L. McGregor.** 1974. Micromanipulation of the flagellum of *Crithidia oncopelti*. I. Mechanical effects. J. Exp. Biol. **60:**437–444.
23. **Holwill, M. E., and J. L. McGregor.** 1975. Control of flagellar wave movement in *Crithidia oncopelti*. Nature **255:**157–158.
24. **Holwill, M. E., and J. L. McGregor.** 1976. Effects of calcium on flagellar movement in the trypanosome *Crithidia oncopelti*. J. Exp. Biol. **65:**229–242.
25. **Imboden, M., N. Muller, A. Hemphill, R. Mattioli, and T. Seebeck.** 1995. Repetitive proteins from the flagellar cytoskeleton of African trypanosomes are diagnostically useful antigens. Parasitology **110:**249–258.
26. **Ismach, R., C. M. Cianci, J. P. Caulfield, P. J. Langer, A. Hein, and D. McMahon-Pratt.** 1989. Flagellar membrane and paraxial rod proteins of *Leishmania:* characterization employing monoclonal antibodies. J. Protozool. **36:**617–624.
27. **Kohl, L., T. Sherwin, and K. Gull.** 1999. Assembly of the paraflagellar rod and the flagellum attachment zone complex during the *Trypanosoma brucei* cell cycle. J. Eukaryot. Microbiol. **46:**105–109.
28. **Maga, J. A., and J. H. LeBowitz.** 1999. Unravelling the kinetoplastid paraflagellar rod. Trends Cell Biol. **9:**409–413.
29. **Maga, J. A., T. Sherwin, S. Francis, K. Gull, and J. H. LeBowitz.** 1999. Genetic dissection of the *Leishmania* paraflagellar rod, a unique flagellar cytoskeleton structure. J. Cell Sci. **112:**2753–2763.
30. **Moreira-Leite, F. F., W. de Souza, and N. L. da Cunha-e-Silva.** 1999. Purification of the paraflagellar rod of the trypanosomatid *Herpetomonas megaseliae* and identification of some of its minor components. Mol. Biochem. Parasitol. **104:**131–140.
31. **Moreira-Leite, F. F., T. Sherwin, L. Kohl, and K. Gull.** 2001. A trypanosome structure involved in transmitting cytoplasmic information during cell division. Science **294:**587–591.
32. **Mundim, M. H., I. Roitman, M. A. Hyermans, and E. W. Kitajima.** 1974. Simple nutrition of *Crithidia deanei*, a reduvid trypanosomatid with an endosymbiont. J. Protozool. **21:**518–521.
33. **Novak, E., E. F. Haapalainem, S. Silva, and J. F. Silveira.** 1988. Protein synthesis in isolated symbiont from the flagellate protozoon *Crithidia deanei*. J. Protozool. **35:**375–378.
34. **Pullen, T. J., M. L. Ginger, S. J. Gaskell, and K. Gull.** 2004. Protein targeting of an unusual, evolutionary conserved adenylate kinase to a eukaryotic flagellum. Mol. Biol. Cell **15:**3257–3265.
35. **Ridgley, E., P. Webster, C. Patton, and L. Ruben.** 2000. Calmodulin-binding properties of the paraflagellar rod complex from *Trypanosoma brucei*. Mol. Biochem. Parasitol. **109:**195–201.
36. **Sambrook, J., and D. W. Russell.** 2001. Molecular cloning: a laboratory manual, 3rd ed. Cold Spring Harbor Laboratory Press, Cold Spring Harbor, NY.
37. **Santrich, C., L. Moore, T. Sherwin, P. Bastin, C. Brokaw, K. Gull, and J. H. LeBowitz.** 1997. A motility function for the paraflagellar rod of *Leishmania* parasites revealed by PFR-2 gene knockouts. Mol. Biochem. Parasitol. **90:**95–109.
38. **Schlaeppi, K., J. Deflorin, and T. Seebeck.** 1989. The major component of the paraflagellar rod of *Trypanosoma brucei* is a helical protein that is encoded by two identical, tandemly linked genes. J. Cell Biol. **109:**1695–1709.
39. **Sugrue, P., M. R. Hirons, J. U. Adam, and M. E. Holwill.** 1988. Flagellar wave reversal in the kinetoplastid flagellate *Crithidia oncopelti*. Biol. Cell **63:**127–1331.
40. **Tetaud, E., I. Lecuix, T. Sheldrake, T. Baltz, and A. H. Fairlamb.** 2002. A new expression vector for *Crithidia fasciculata* and *Leishmania*. Mol. Biochem. Parasitol. **120:**195–204.
41. **Tetley, L., and K. Vickerman.** 1985. Differentiation in *Trypanosoma brucei:* host-parasite cell junctions and their persistence during acquisition of the variable antigen coat. J. Cell Sci. **74:**1–19.
42. **Vickerman, K.** 1994. The evolutionary expansion of the trypanosomatid flagellates. Int. J. Parasitol. **24:**1317–1331.
43. **Wickstead, B., K. Ersfeld, and K. Gull.** 2004. The small chromosomes of *Trypanosoma brucei* involved in antigenic variation are constructed around repetitive palindromes. Genome Res. **14:**1014–1024.
44. **Woodward, R., M. J. Carden, and K. Gull.** 1994. Molecular characterization of a novel, repetitive protein of the paraflagellar rod in *Trypanosoma brucei*. Mol. Biochem. Parasitol. **67:**31–39.